Atmos. Chem. Phys. Discuss., 11, 28563–28586, 2011
www.atmos-chem-phys-discuss.net/11/28563/2011/
doi:10.5194/acpd-11-28563-2011
© Author(s) 2011. CC Attribution 3.0 License.

Atmospheric Chemistry and Physics Discussions

This discussion paper is/has been under review for the journal Atmospheric Chemistry and Physics (ACP). Please refer to the corresponding final paper in ACP if available.

Importance of atmospheric aging in reactivity of mineral dust aerosol: a case study of heterogeneous reaction of gaseous hydrogen peroxide on processed mineral particles

Y. Zhao, Z. M. Chen, X. L. Shen, and D. Huang

State Key Laboratory of Environmental Simulation and Pollution Control, College of Environmental Sciences and Engineering, Peking University, Beijing 100871, China

Received: 20 September 2011 – Accepted: 12 October 2011 – Published: 24 October 2011

Correspondence to: Z. M. Chen (zmchen@pku.edu.cn)

Published by Copernicus Publications on behalf of the European Geosciences Union.

Abstract

Atmospheric aging and processing appears to alter physical and chemical properties of mineral dust aerosol and thus its role as reactive surface in the troposphere. Yet, previous studies in the atmosphere have mainly focused on the clean surfaces of mineral dust aerosol, and the reactivity of aged mineral aerosol toward atmospheric trace gases is still poorly recognized. This work presents the first laboratory investigation of heterogeneous reactions of gaseous hydrogen peroxide (H_2O_2), an important atmospheric oxidant, on the surface of HNO_3 and SO_2-processed alumina particles as surrogates of mineral dust aerosol aged by acidic trace gases as a function of relative humidity (RH) and surface coverage of coatings. Pretreatment of the alumina surfaces with HNO_3 and SO_2 has a strong impact on its reactivity toward H_2O_2 uptake. On HNO_3-processed particles, because of the dual role of the nitrate coating in modifying the reactivity of the particle surface, namely blocking oxide active sites but altering surface hygroscopicity, H_2O_2 uptake seems to decrease in some cases whereas increase in other cases, largely depending on RH and surface coverage of nitrate. On SO_2-processed particles, the presence of adsorbed S(IV) species appears to enhance the intrinsic reactivity of the alumina particles due to its affinity for H_2O_2, and the uptake of H_2O_2 increases by 40–80 % in the range of RH from 25 % to 92 % relative to the unprocessed particles. However, when S(IV) is completely oxidized to S(VI), the alumina surface is significantly deactivated and the measured uptake of H_2O_2 decreased markedly. The mechanisms for heterogeneous reactions of H_2O_2 with these processed particles are discussed, as well as its potential implications on tropospheric chemistry. The results of our study suggest that the reactivity of mineral dust aerosol toward H_2O_2 and maybe other atmospheric trace gases will depend on the chemical nature and coverage of the coatings as well as ambient RH, and thus will vary considerably in different polluted atmosphere, which should be taken into account in current atmospheric models.

ACPD

11, 28563–28586, 2011

1 Introduction

Mineral dust aerosol constitutes a significant fraction of atmospheric particulate matter, playing an important role in atmospheric environment and climate change (Dentener et al., 1996; Sokolik and Toon, 1996; Prospero, 1999; Buseck and Posfai, 1999; Ndour et al., 2008). As a reactive surface in the global troposphere, mineral dust aerosol can interact with a variety of trace gases during atmospheric transport (Dentener et al., 1996; Usher et al., 2003a). Laboratory studies have shown that heterogeneous reaction of trace gases including HNO_3, oxides of nitrogen and sulfur, and volatile organic compounds on mineral dust and its components generally leads to the formation of some low-volatile and/or nonvolatile products, such as nitrate, sulfate, and oxidized organics, on particle surfaces (Usher et al., 2003a; Crowley et al., 2010; Kolb et al., 2011). Field observations have also revealed that atmospheric mineral dust aerosol, through heterogeneous uptake of acidic gases and organic compounds, often accumulate nitrate, sulfate, as well as organic coatings (Buseck and Posfai, 1999; Falkovich et al., 2004; Putaud et al., 2004; Sullivan et al., 2007; Li et al., 2009; Formenti et al., 2011). These inorganic or organic coatings have been expected to alter physical and chemical properties of mineral dust aerosol and thus its role as a reactive surface in the downstream atmosphere. Therefore, it is an important issue to characterize the reactivity of mineral dust aerosol processed or aged by interacting with atmospheric trace gases. However, few studies on heterogeneous atmospheric chemistry have focused on the aged mineral aerosol particles. Usher et al. (2003b) have reported the reactive uptake of ozone on mineral oxide particles coated in nitrate, sulfate, as well as organics under dry conditions, and found that the uptake of ozone by processed particles could be increased or decreased relative to the uncoated particles, depending on the molecular nature of the coating. Recently, it has been shown that the photolysis of adsorbed nitrate on alumina under atmospherically relevant conditions can significantly yield NO_2 (Schuttlefield et al., 2008) and that irradiation of NO_2-reacted alumina particles can lead to the oxidation of adsorbed organic compounds (Raff et al., 2011). Nonetheless, information

ACPD
11, 28563–28586, 2011

regarding the reactivity of aged mineral aerosols toward atmospheric trace gases is still quite limited. In addition, little is know about the associated kinetics under humid conditions that are more relevant to the real troposphere.

Hydrogen peroxide (H_2O_2) is an important atmospheric oxidant, playing an important role in secondary sulfate formation and HO_x radical chemistry (Finlayson-Pitts and Pitts, 2000; Reeves and Penkett, 2003; Hua et al., 2008). Field studies have shown that heterogeneous reactions on ambient mineral aerosol (De Reus et al., 2005) and urban aerosols (He et al., 2010) seem to be an important sink for gaseous H_2O_2. Accordingly, recent several laboratory studies have reported the kinetics and mechanisms of the interaction of H_2O_2 with the clean surface of mineral dust aerosol and its components (Pradhan et al., 2010a, b; Zhao et al., 2011). However, the reactivity of aged mineral aerosol toward H_2O_2 is still unclear.

The aim of this study is to probe the effect of atmospheric aging on the reactivity of mineral aerosol by investigating H_2O_2 uptake on HNO_3 and SO_2-processed alumina particles. Here, alumina was selected as a substrate as a result of its abundance in atmospheric mineral aerosol and its affinity for acidic trace gases. A full range of relative humidity (RH) conditions as well as surface coverage of coatings (to simulate different degree of atmospheric aging) was considered to explore their effects on the uptake of H_2O_2. It is found that the reactivity of alumina particles toward H_2O_2 is significantly modified due to the pretreatment with HNO_3 or SO_2, with a striking dependence on RH and the degree of aging.

2 Experimental

2.1 Preparation of HNO_3 and SO_2 processed α-Al_2O_3

The processed particle samples were prepared in a flow reactor which has been described previously (Chen et al., 2008). Briefly, the flow reactor (length 15 cm, ID 3.3 cm) is a quartz cylinder. The α-Al_2O_3 powder (Alfa Aesar, Brunauer-Emmett-Teller (BET)

ACPD
11, 28563–28586, 2011

surface area of 32.8 $m^2 g^{-1}$), with typical sample mass of 15 mg, was directly placed on a 250 mesh stainless steel circular grid and compressed to form a solid coating, which was then mounted in the center of the reactor. Before exposure to HNO_3 or SO_2, the particle sample was evacuated at 298 K for at least 60 min to remove the physisorbed impurities as much as possible. The HNO_3 or SO_2-containing simulated air (400 sccm) was then introduced into the reactor. To assuring a relative large reactivity of alumina particles toward HNO_3 and SO_2, the humidity of HNO_3 and SO_2-containing airflow was controlled at 35 % RH and <1 % RH, respectively. Previous studies (Boerensen et al., 2000; Hanisch and Crowley, 2001; Goodman et al., 2001a, b; Usher et al., 2002) have shown that HNO_3 and SO_2 can irreversibly react with Al_2O_3 to form surface-bound nitrate and sulfite (and/or bisulfite) species, respectively. In order to evaluate the impact of the degree of aging on heterogeneous chemistry of α-Al_2O_3, different coverages of nitrate and sulfite (and/or bisulfite) coatings were obtained by varying exposure time. During the laboratory-simulated aging processes, a FTIR spectrometer (Nicolet 6700, Thermo Scientific) coupled to the flow reactor was also employed to record the infrared spectra of the particle samples in the transmission mode in the frequency range of 4000 to 400 cm^{-1}. All spectra were collected at a resolution of 4 cm^{-1}, and 64 scans were averaged for each spectrum corresponding to a time resolution of 39 s.

2.2 H_2O_2 uptake experiments

After reaction with HNO_3 or SO_2, the α-Al_2O_3 samples were evacuated for at least 2 hours to remove physisorbed HNO_3 or SO_2. Subsequently, the H_2O_2-containing simulated air was introduced into the reactor at a constant flow rate of 400 sccm, ensuring a laminar regime. Uptake experiments were performed under different wet conditions, varying from dry conditions (3 % RH) and up to 92 % RH. The RH was measured by a hygrometer (Vaisala HMT100) with the uncertainty of ±1.7 %. T-FTIR spectra of the particle samples were recorded upon H_2O_2 uptake. Each spectrum was referenced to the spectrum of particles saturated with H_2O_2-free simulated air at the same RH.

ACPD
11, 28563–28586, 2011

At the exit of the flow reactor, the 400 sccm air stream was drawn into a thermostatically controlled scrubbing coil collector maintained at 277 ± 0.2 K, and the 1 mM H_3PO_4 solution (prepared by 85 % aqueous solution for HPLC, Sigma-Aldrich), used as the stripping solution, was delivered into the collector by a peristaltic pump at a flow rate of 0.2 ml min^{-1} to collect the gas-phase H_2O_2. The resulting solution was then immediately analyzed with a HPLC instrument described below. By subtracting the gas-phase H_2O_2 loss in the absence of particles (namely the wall loss) from that in the presence of particles, the uptake of H_2O_2 by particles can be derived. The collection efficiency of the coil for H_2O_2 was determined to be ≥98 % (Hua et al., 2008), and further details about this collection system can be seen in our previous work (Hua et al., 2008). A typical uptake experiment lasted 30 min for HNO_3-processed particles and 60 min for SO_2-processed particles, and during all uptake experiments the flow reactor was maintained at 298 ± 1 K and ambient pressure.

After reaction with H_2O_2, the particle sample was sonicated in 10 ml Milli-Q water (Millipore, USA) to extract surface adsorbed nitrate and sulfate. The resulting solution was then filtered and analyzed using an ion chromatography (Dionex ICS2000, USA), which is equipped with a Dionex AS 11 analytical column and a conductivity detector. The number of surface-bound sulfite/bisulfite on α-Al_2O_3 pretreated with SO_2 was also obtained assuming all of S(IV) species were oxidized to sulfate by H_2O_2.

Based on the uptake rate ($d\{C\}/dt$) of H_2O_2, which was determined from the linear fit to the time-dependent uptake data within 10 min of exposure, the uptake coefficients of H_2O_2 on processed particles were calculated.

$$\gamma = \frac{d\{C\}/dt}{Z} \tag{1}$$

$$Z = \frac{1}{4} A_s [C] \sqrt{\frac{8RT}{\pi M_c}} \tag{2}$$

where $\{C\}$ is the uptake of H_2O_2 by particle surfaces, Z is collision frequency of gas-phase H_2O_2 with the particle surface, $[C]$ is the gas-phase H_2O_2 concentration, M_c is

ACPD
11, 28563–28586, 2011

the molecular weight of H_2O_2, and A_s is the effective surface area of the particle samples. As reported in our previous work (Zhao et al., 2011), the measured BET uptake coefficient of H_2O_2 on bulk alumina powder sample is independent of the sample mass, suggesting that the BET surface area appears to more appropriately represent the effective surface area of the sample. It should be noted that the uptake experiments were performed at relative high H_2O_2 pressures to enable IR observation of surface species on the particle sample, and on a few minutes timescale the initial uptake processes are already achieved. Therefore, the measured uptake coefficients in this study represent the steady state rather than the initial state.

2.3 Generation of gaseous H_2O_2

The commercial H_2O_2 solution (Sigma-Aldrich, 50 wt %) was concentrated in a bubbler by bubbling 100 sccm dry N_2 through it at 277 ± 0.2 K for 4 days. A few milliliters of the concentrated H_2O_2 solution were then transferred to another bubbler at 277 ± 0.2 K and a dry N_2 flow of 20 sccm was bubbled through the solution. The resulting N_2 flow was then balanced with 380 sccm of simulated air before being introduced into the reactor to give a typical gaseous H_2O_2 concentration of 1.7×10^{14} molecules cm^{-3}.

2.4 H_2O_2 detection

H_2O_2 was determined using a HPLC instrument (Agilent 1200, USA) equipped with a fluorescent detector, with post-column derivation involving the hemin-catalyzed oxidation of H_2O_2 to a fluorescent derivative by hydroxyphenylacetic acid. Further detail about the method can be found in our previous study (Hua et al., 2008).

ACPD
11, 28563–28586, 2011

3 Results and discussion

3.1 H_2O_2 uptake on HNO_3 processed particles

H_2O_2 uptake on clean α-Al_2O_3 particles has been studied in our previous work (Zhao et al., 2011). It was found that H_2O_2 molecules mainly undergo catalytic decomposition on the surface but also a small amount of molecularly adsorbed H_2O_2 can be observed. Here the effect of HNO_3-processing on the reactivity of α-Al_2O_3 particles toward $H_2O_2$was investigated as a function of RH and surface nitrate coverage. The RH considered here ranges from 3 % and up to 92 %, covering the RH prevailed in most atmospheric environments. The surface coverage of nitrate varies from 0 to 3.5×10^{18} molecules m^{-2}, to simulate varying degrees of atmospheric aging of mineral particles by HNO_3 and other nitrogen species. Given the radius of surface-coordinated nitrate ion of 126 pm (Greenwood and Earnshaw, 1997), adsorbed nitrate would cover approximately 0–18 % monolayer of the BET surface.

Figure 1 shows T-FTIR spectra of HNO_3-processed alumina particles following exposure to 1.7×10^{14} molecules cm^{-3} gaseous H_2O_2. The spectrum of H_2O_2 uptake on clean α-Al_2O_3 was also displayed for comparison. The absorption bands at 3209 cm^{-1}, 2805 cm^{-1}, 1426 cm^{-1}, 1332 cm^{-1} are ascribed to the characteristic vibrations of the molecularly adsorbed H_2O_2 (Zhao et al., 2011). For nitrate-coated particles, the absorption bands at 1426 cm^{-1} and 1332 cm^{-1} are overlapping with the bands due to surface water-solvated nitrate ions (Goodman et al., 2001b). It is notable that with the increase of surface coverage of nitrate coating, the amount of molecularly adsorbed H_2O_2 on α-Al_2O_3 decreases markedly at 3 % RH whereas increases slightly at 92% RH, implying that the pretreatment of α-Al_2O_3 with HNO_3 appears to have distinct impacts on the reactivity of particles toward H_2O_2 under different humidity conditions.

The reactivity of HNO_3-processed α-Al_2O_3 particles toward H_2O_2 uptake can be further characterized in term of the uptake coefficients. Figure 2 shows H_2O_2 uptake on HNO_3-processed alumina particles as a function of RH and surface nitrate coverage.

ACPD
11, 28563–28586, 2011

As a comparison, the uptake of H_2O_2 on clean α-Al_2O_3 at varying RH was also measured in this study. The values of the uptake coefficients measured here are in good agreement with those reported previously (Zhao et al., 2011). It is evident from Fig. 2 that H_2O_2 uptake on HNO_3-processed alumina particles greatly differs from that on unprocessed particles, with a striking dependence on RH and surface coverage of nitrate. As suggested previously (Zhao et al., 2011), the catalytic decomposition as well as molecular adsorption at oxide active sites contributes to H_2O_2 uptake on alumina surfaces. The HNO_3 reaction with alumina appears to consume the same surface sites for H_2O_2 uptake, leading to the decrease of surface reactivity. However, the nitrate coating can largely enhance the surface hygroscopicity and thus water uptake of alumina surfaces under wet conditions, which may favor H_2O_2 uptake onto surface liquid-like water in particular at high RH due to the high solubility of H_2O_2. Therefore, the HNO_3-processing seems to play dual roles in modifying reactivity of alumina particles toward H_2O_2, either by consuming surface oxide active sites or by increasing surface hygroscopicity. Obviously, the relative importance of these two mechanisms finally determines the net effect of HNO_3-processing on H_2O_2 uptake on alumina particles.

Under dry conditions, the quantity of oxide active sites determines the reactivity of α-Al_2O_3 toward H_2O_2. Thus, by occupying surface reactive sites, adsorbed nitrate on α-Al_2O_3 is expected to decrease the reactivity of the surface. As shown here, at 3 % RH, the measured uptake of H_2O_2 on processed α-Al_2O_3 decreases from 1.1×10^{-7} to 0.7×10^{-7} with the surface nitrate coverage increasing from 0 to 3.5×10^{18} molecules m^{-2}. Similar deactivation of α-Al_2O_3 surfaces with adsorbed nitrate was also observed in the study performed by Usher et al. (2003b), with O_3 uptake on nitrated α-Al_2O_3 under dry conditions decreasing by approximately 70% relative to that on unprocessed particles. At intermediate RH (25–60 %), the presence of adsorbed nitrate at low surface coverage still decreases the reactivity of alumina particles toward H_2O_2 by blocking surface reactive sites. However, as the surface nitrate coverage increases the particle surfaces become more hydrophilic. The surface reactivation attributed to the increase of surface hygroscopicity prevails against the further deactivation of the

ACPD
11, 28563–28586, 2011

particles due to the occupation of surface reactive sites by adsorbed nitrate, finally leading to the recovery of surface reactivity toward H_2O_2. Therefore, as the surface nitrate coverage increases, a turning point for H_2O_2 uptake is expected. As shown in Fig. 2, the measured uptake coefficient of H_2O_2 on HNO_3-processed alumina particles initially decreases and then increases with the surface coverage of nitrate. It is interesting to note that at RH of 25–60 % and surface nitrate coverage higher than 3.0×10^{18} molecules m^{-2}, the measured uptake of H_2O_2 is equivalent to or even larger than that on the unprocessed particles. At high RH (75–92 %), the presence of nitrate coatings strongly enhances the coverage of liquid-like water on the surface. Thus, via adsorption into the growing islands of liquid-like water, H_2O_2 uptake increases with increasing nitrate coverage.

3.2 H_2O_2 uptake on SO_2 processed particles

It has been shown that SO_2 can interact with alumina particles to form surface-coordinated sulfite and/or bisulfite species (Goodman et al., 2001a; Usher et al., 2002). As an efficient oxidant for sulfate formation in cloud water and on ice surfaces (Finlayson-Pitts and Pitts, 2000; Chu et al., 2000; Clegg and Abbatt, 2001), H_2O_2 may also have the potential to oxidize S(IV) species to S(VI) on the surface of mineral particles. The SO_2-processed alumina is therefore expected to have different reactivity toward H_2O_2 compared to the HNO_3-processed particles. In this study, the surface coverage of sulfite/bisulfite was determined to be $(8.6 \pm 1.0) \times 10^{17}$ molecules m^{-2}. With the sulfite ion radius of 151 pm (Greenwood and Earnshaw, 1997), surface-coordinated S(IV) would cover approximately 6.2 % of the BET surface of alumina particles.

Figure 3a shows the T-FTIR spectra of the SO_2-processed particles collected upon exposure to gaseous H_2O_2 at 3 % RH. The absorption bands at 1161 cm^{-1} and 1059 cm^{-1}, assigned to surface-bound sulfate and/or bisulfate (Fu et al., 2007), significantly increase in intensity with exposure time, suggesting that H_2O_2 can efficiently oxidize adsorbed sulfite/bisulfite to sulfate/bisulfate on alumina surfaces. The mechanism of this oxidation can be described as follows:

ACPD
11, 28563–28586, 2011

$$SO^{2-}_{3(ads)} + H_2O_{2(ads)} \rightarrow SO^{2-}_{4(ads)} + H_2O \quad \text{(R1)}$$

$$HSO^{-}_{3(ads)} + H_2O_{2(ads)} \rightarrow HSO^{-}_{4(ads)} + H_2O \quad \text{(R2)}$$

After 30 min of exposure, about 90 % of surface S(IV) species is converted to S(VI) that is relatively inactive toward H_2O_2, and several new absorption bands at 3209 cm^{-1}, 2805 cm^{-1}, and between 1500 and 1300 cm^{-1}, associated with the molecularly adsorbed H_2O_2 (Zhao et al., 2011), appear and grow in intensity with exposure time. Similar T-FTIR experiments upon varying RH were also carried out to probe the effect of water on H_2O_2 uptake on processed particles. Figure 3b shows the T-FTIR spectra following the reaction of H_2O_2 with SO_2-processed alumina particles at 45 % RH. The absorption bands at 1161 cm^{-1} and 1059 cm^{-1} due to surface-bound sulfate observed at 3 % RH combines into one band at 1139 cm^{-1} at 45 % RH. This frequency shift is probably owing to water-solvation effects of sulfate, which was also observed for nitrate on alumina surfaces. It is evident that sulfate formation on the surface at 45 % RH is fast relative to that at 3 % RH, revealing that water can substantially promote the oxidation of S(IV) by H_2O_2. Similarly, when almost all of the S(IV) species are oxidized to S(VI), the molecularly adsorbed H_2O_2 appears on the particle surface.

In addition, the uptake of H_2O_2 was determined to further explore the reactivity of SO_2-processed alumina particles. The insets in Fig. 3 show the temporal evolution of H_2O_2 uptake on processed particles. According to the chemical nature of particle surfaces, the whole uptake processes were separated into two stages. During the stage I, surface S(IV) species efficiently react with H_2O_2 to form sulfate; As for stage II, the oxidation of surface S(IV) species is almost completed, and the alumina particles are coated with sulfate. Based on linear fits to the measured H_2O_2 uptake within the first 10 min of exposure for each stage, the uptake coefficient (γ) of H_2O_2 on SO_2-processed particles was calculated using Eqs. (1) and (2). Figure 4 illustrates the γ of H_2O_2 on SO_2-processed particles as a function of RH, and the uptake coefficient of H_2O_2 on unprocessed alumina particles was also displayed for comparison. It can

ACPD
11, 28563–28586, 2011

be seen that at 3 % RH, there is a slight increase (about 5 %) in H_2O_2 uptake on SO_2-processed particles. As RH increases, this enhancement of H_2O_2 uptake becomes striking, ranging from 40 % at 25 % RH to 72 % at 92 % RH. This indicates that the presence of surface S(IV) species can enhance the reactivity of alumina particles toward H_2O_2, in particular under humid conditions. However, after surface S(IV) species are converted to S(VI), the particle surfaces become less reactive and H_2O_2 uptake decreases markedly. Similar to the surface adsorbed nitrate, the sulfate coating also has dual impacts on the reactivity of alumina surfaces, namely blocking oxide active sites but altering surface hygroscopicity. Thus, the reactivity of sulfate-coated alumina particles toward H_2O_2 is also expected to depend on the surface coverage of sulfate and RH. As shown here, the presence of sulfate at coverage of 8.6×10^{17} molecules m^{-2} on the surface of alumina decreases the uptake of H_2O_2 at RH <60 % whereas enhances H_2O_2 uptake at RH >60 %.

Since only 6.2 % of the BET surface of alumina particles that has been pretreated with SO_2 is covered by a monolayer of S(IV) species, the measured uptake of H_2O_2 on SO_2-processed particles has contributions from the uptake on both adsorbed sulfite/bisulfite sites and uncovered oxide active sites. Thus, H_2O_2 uptake on SO_2-processed particles can be expressed as:

$$\gamma_{\text{processed}} = \sum f_i \gamma_i = \gamma_{(\text{absorbate active sites})} + \gamma_{(\text{oxide active sites})} \quad (3)$$

where f_i and γ_i are the fraction and the measured uptake respectively for each of these sites (Usher et al., 2003b). Based on surface coverage of S(IV) species and the measured uptake coefficients on processed and unprocessed particles (Fig. 4), H_2O_2 uptake due to the oxidation of S(IV) at varying RH can be estimated. As shown in Fig. 5, the probability of oxidation of S(IV) to S(VI) by H_2O_2, $\gamma_{S(IV)}$, increases from $(1.9 \pm 0.5) \times 10^{-7}$ to $(8.3 \pm 0.5) \times 10^{-7}$ with increasing RH in the range from 3 % to 92 %, nearly twice to decuple H_2O_2 uptake on uncovered oxide active sites of alumina. This marked positive correlation between $\gamma_{S(IV)}$ and RH also evidently indicates water-enhanced oxidation of S(IV) by H_2O_2. Generally, the rate law for the oxidation of S(IV)

ACPD
11, 28563–28586, 2011

by H_2O_2 can be expressed by the equation (Finlayson-Pitts and Pitts, 2000):

$$-\frac{d[\mathrm{S(IV)}]}{dt} = k\left[\mathrm{H^+}\right][\mathrm{H_2O_2}][\mathrm{S(IV)}] \quad (4)$$

Under humid conditions, water adsorption on particle surfaces inhibits catalytic decomposition of accommodated H_2O_2 on uncovered oxide active sites of SO_2-processed alumina particles (Zhao et al., 2011), thus resulting in a relatively large concentration of H_2O_2 available for the oxidation of S(IV). In addition, adsorbed water can facilitate the dissociation of surface-bound bisulfate, which is suggested by IR absorption associated with water-solvated sulfate ions at 45% RH (Fig. 3), to yield free H^+ ions on the surface. These changes in microenvironments of the particle surface due to adsorbed water appear to rationalize our observations.

It has been recently reported that O_3 could promote the conversion of S(IV) species to S(VI) on mineral dust particles (Ullerstam et al., 2002; Usher et al., 2002; Li et al., 2006). Usher at al. (2003b) have investigated O_3 uptake on α-Al_2O_3 particles pretreated with SO_2 using Knudsen cell reactor, and suggested the probabililty of O_3 uptake on S(IV)-covering sites on alumina particles is double that on the uncovered sites. Given the BET uptake coefficients of $(3.5 \pm 0.9) \times 10^{-8}$ for O_3 on untreated alumina particles at RH ≤ 1 % calculated from time dependent IR signals due to O_3 decay (Mogili et al., 2006), the probability of oxidation of adsorbed S(IV) to S(VI) by O_3 is estimated to be 7.0×10^{-8}, less than half of that by H_2O_2. This reveals that H_2O_2 seems to be more reactive toward adsorbed S(IV) on mineral particles relative to O_3.

4 Conclusions and atmospheric implications

Here heterogeneous reactions of H_2O_2 on alumina particles that have been processed by exposure to gaseous HNO_3 or SO_2, as proxies of ambient mineral aerosol aged by acidic trace gases, were investigated as a function of RH and surface coverage of coatings. The uptake kinetics of H_2O_2 on clean surfaces of mineral dust aerosol and its components has been reported in recent studies by Pradhan et al. (2010a, b)

ACPD
11, 28563–28586, 2011

and in our previous work (Zhao et al., 2011). For suspended TiO_2, Gobi sand, and Saharan dust aerosols in an aerosol flow tube (AFT), the uptake coefficients (γ) of H_2O_2can get up to 10^{-4} (Pradhan et al., 2010a, b), whereas for bulk alumina powder samples, the uptake coefficients are on the order of 10^{-7} (Zhao et al., 2011). This large discrepancy in γ, as discussed previously (Zhao et al., 2011), is mainly due to the different experimental techniques employed, different sample treatments, and different H_2O_2 pressures used. Since AFT can achieve the most realistic conditions of atmospheric aerosol, the H_2O_2 uptake coefficient on the order of 10^{-4} obtained with this method is considered as preferred value (Crowley et al., 2010). In light of this, we may be able to tentatively extrapolate the uptake coefficient determined using our experimental apparatus to the real atmosphere by multiplying approximately three orders of magnitude. The value of uptake coefficient on the order of 10^{-4} suggests that the uptake of H_2O_2 by clean surfaces of mineral dust aerosol can be an important sink for tropospheric H_2O_2 (Pradhan et al., 2010b). However, during atmospheric transport, the reactivity of mineral dust aerosol is likely to be modified by other traces gases in the troposphere. In this study, the measured uptake data can basically reflect the effect of atmospheric aging on the reactivity of mineral aerosol toward H_2O_2. It is found that atmospheric aging has a strong impact on the reactivity of mineral aerosol toward H_2O_2 uptake. For example, at typical RH values of the troposphere (20–90 %), mineral particles accumulating a coating of sulfite at coverage of 8.6×10^{17} molecules m^{-2} will exhibit an enhanced H_2O_2 uptake by 40–80 % relative to the clean particles, and in the cases of higher aging degree the enhancement of the reactivity is expected to be more significant. However, when mineral particles are coated with nitrate or sulfate, the uptake of H_2O_2 will decrease at low RH (<25 %) whereas increase at high RH (75–90 %), and at intermediate RH (25–60 %) the effect of the coating is intimately related to its surface coverage. Thus, the loss of H_2O_2 due to uptake onto atmospheric mineral dust aerosol will depend on the molecular nature and the coverage of surface materials, as well as ambient RH, and hence will vary considerably in different polluted environments.

ACPD
11, 28563–28586, 2011

It should be noted that the HNO_3 and SO_2-processed alumina particles used in this study to simulate the effects of atmospheric aging are simple models for ambient aged mineral aerosols. For example, the several layers of nitrate coatings could be observed on mineral aerosols in polluted urban atmosphere (Li et al., 2009). However, given that the presence of hydrophilic nitrate coating at surface coverage higher than 3.0×10^{18} molecules m^{-2} (corresponding to approximately 15% monolayer) seems to increase the reactivity of mineral particles toward H_2O_2 uptake under atmospheric relevant conditions (20–90 % RH) due to enhancing surface hygroscopicity (Fig. 2), the thicker coatings of nitrate on aged mineral aerosols observed in the troposphere are expected to enhance the reactivity of the particle surface to a greater extent.

Furthermore, H_2O_2 seems to facilitate heterogeneous sulfate formation on mineral dust aerosols particularly under humid conditions, with mechanisms analogous to secondary sulfate formation in cloud water and on ice surfaces. The sulfate formation on mineral dust in turn affects the physicochemical properties of particles, altering the hygroscopicity, the ability to act as cloud concentration nuclei or ice nuclei, as well as the reactivity toward various atmospheric trace gases. In addition, catalytic decomposition of H_2O_2 at uncovered active sites of mineral particles as well as the direct photolysis of the molecularly adsorbed H_2O_2 can generate hydroxyl radicals (Zhao et al., 2011), which may also favor the oxidation of organic compounds adsorbed or condensed on mineral aerosols. Moreover, the presence of acidic sulfate coating on the surface can possibly lead to the formation of organosulfate species, probably via mechanisms including acid-catalysis and, in the daytime, sulfate radical-initiation (Surratt et al., 2010; Hatch et al., 2011). All of these potentially important issues may further highlight the importance of the interactions between H_2O_2 and aged atmospheric mineral particles and warrant further investigations.

Obviously, in addition to H_2O_2, the interactions of aged mineral aerosol with other atmospheric oxidants such as O_3, OH radicals, and NO_3 radicals may need to be evaluated. It is notable that these interactions may have the potential to significantly alter the oxidative capacity of the atmosphere.

ACPD
11, 28563–28586, 2011

Acknowledgements. The authors gratefully thank the National Natural Science Foundation of China (grants 40875072 and 21077003) and the State Key Laboratory of Environment Simulation and Pollution Control (special fund) for financial support.

References

Borensen, C., Kirchner, U., Scheer, V., Vogt, R., and Zellner, R.: Mechanism and kinetics of the reactions of NO_2 or HNO_3 with alumina as a mineral dust model compound, J. Phys. Chem. A, 104, 5036–5045, 2000.

Buseck, P. R. and Posfai, M.: Airborne minerals and related aerosol particles: Effects on climate and the environment, Proc. Natl. Acad. Sci. USA, 96, 3372–3379, 1999.

Chen, Z. M., Jie, C. Y., Li, S., Wang, C. X., Xu, J. R., and Hua, W.: Heterogeneous reactions of methacrolein and methyl vinyl ketone: Kinetics and mechanisms of uptake and ozonolysis on silicon dioxide, J. Geophys. Res., 113, D22303, doi:10.1029/2007JD009754, 2008.

Chu, L., Diao, G. W., and Chu, L. T.: Heterogeneous Interaction of SO_2 on H_2O_2-Ice Films at 190–210 K, J. Phys. Chem. A, 104, 7565–7573, 2000.

Clegg, S. M. and Abbatt, J. P. D.: Oxidation of SO_2 by H_2O_2 on ice surfaces at 228 K: a sink for SO_2 in ice clouds, Atmos. Chem. Phys., 1, 73–78, doi:10.5194/acp-1-73-2001, 2001.

Crowley, J. N., Ammann, M., Cox, R. A., Hynes, R. G., Jenkin, M. E., Mellouki, A., Rossi, M. J., Troe, J., and Wallington, T. J.: Evaluated kinetic and photochemical data for atmospheric chemistry: Volume V – heterogeneous reactions on solid substrates, Atmos. Chem. Phys., 10, 9059–9223, doi:10.5194/acp-10-9059-2010, 2010.

de Reus, M., Fischer, H., Sander, R., Gros, V., Kormann, R., Salisbury, G., Van Dingenen, R., Williams, J., Zllner, M., and Lelieveld, J.: Observations and model calculations of trace gas scavenging in a dense Saharan dust plume during MINATROC, Atmos. Chem. Phys., 5, 1787–1803, doi:10.5194/acp-5-1787-2005, 2005.

Dentener, F. J., Carmichael, G. R., Zhang, Y., Leliveld, J., and Crutzen, P. J.: Role of mineral aerosol as a reactive surface in the global troposphere, J. Geophys. Res., 101, 22869–22889, 1996.

Falkovich, A. H., Schkolnik, G., Ganor, E., and Rudich, Y.: Adsorption of organic compounds pertinent to urban environments onto mineral dust particles, J. Geophys. Res., 109, D02208, doi:10.1029/2003JD003919, 2004.

ACPD

11, 28563–28586, 2011

Finlayson-Pitts, B. J. and Pitts, J. N.: Chemistry of the Upper and Lower Atmosphere, Academic Press, New York, 2000.

Formenti, P., Schtz, L., Balkanski, Y., Desboeufs, K., Ebert, M., Kandler, K., Petzold, A., Scheuvens, D., Weinbruch, S., and Zhang, D.: Recent progress in understanding physical and chemical properties of African and Asian mineral dust, Atmos. Chem. Phys., 11, 8231–8256, doi:10.5194/acp-11-8231-2011, 2011.

Fu, H. B., Wang, X., Wu, H. B., Yin, Y., and Chen, J. M.: Heterogeneous Uptake and Oxidation of SO_2 on Iron Oxides, J. Phys. Chem. C, 111, 6077–6085, 2007.

Goodman, A. L., Li, P., Usher, C. R., and Grassian, V. H.: Heterogeneous uptake of sulfur dioxide on aluminum and magnesium oxide particles, J. Phys. Chem. A, 105, 6109–6120, 2001a.

Goodman, A. L., Bernard, E. T., and Grassian, V. H.: Spectroscopic study of nitric acid and water adsorption on Oxide particles: enhanced nitric acid uptake kinetics in the presence of adsorbed water, J. Phys. Chem. A, 105, 6443–6457, 2001b.

Greenwood, N. N. and Earnshaw, A.: Chemistry of the Elements, Second Edition, Butterworth-Heinemann, Oxford, 1997.

Hanisch, F. and Crowley, J. N.: Heterogeneous reactivity of gaseous nitric acid on Al_2O_3, $CaCO_3$, and atmospheric dust samples: A Knudsen cell study, J. Phys. Chem. A, 105, 3096–3106, 2001.

Hatch, L. E., Creamean, J. M., Ault, A. P., Surratt, J. D., Chan, M. N., Seinfeld, J. H., Edgerton, E. S., Su, Y. X., and Prather, K. A: Measurements of Isoprene-Derived Organosulfates in Ambient Aerosols by Aerosol Time-of-Flight Mass Spectrometry – Part 2: Temporal Variability and Formation Mechanisms, Environ. Sci. Technol., 45, 8648-8655, doi:10.1021/es2011836,2011.

He, S. Z., Chen, Z. M., Zhang, X., Zhao, Y., Huang, D. M., Zhao, J. N., Zhu, T., Hu, M., and Zeng, L. M.: Measurement of atmospheric hydrogen peroxide and organic peroxides in Beijing before and during the 2008 Olympic Games: Chemical and physical factors influencing their concentrations, J. Geophys. Res., 115, D17307, doi:10.1029/2009JD013544, 2010.

Hua, W., Chen, Z. M., Jie, C. Y., Kondo, Y., Hofzumahaus, A., Takegawa, N., Chang, C. C., Lu, K. D., Miyazaki, Y., Kita, K., Wang, H. L., Zhang, Y. H., and Hu, M.: Atmospheric hydrogen peroxide and organic hydroperoxides during PRIDE-PRD'06, China: their concentration, formation mechanism and contribution to secondary aerosols, Atmos. Chem. Phys., 8, 6755–6773, doi:10.5194/acp-8-6755-2008, 2008.

ACPD
11, 28563–28586, 2011

Kolb, C. E., Cox, R. A., Abbatt, J. P. D., Ammann, M., Davis, E. J., Donaldson, D. J., Garrett, B. C., George, C., Griffiths, P. T., Hanson, D. R., Kulmala, M., McFiggans, G., Pöschl, U., Riipinen, I., Rossi, M. J., Rudich, Y., Wagner, P. E., Winkler, P. M., Worsnop, D. R., and O' Dowd, C. D.: An overview of current issues in the uptake of atmospheric trace gases by aerosols and clouds, Atmos. Chem. Phys., 10, 10561–10605, doi:10.5194/acp-10-10561-2010, 2010.

Li, L., Chen, Z. M., Zhang, Y. H., Zhu, T., Li, J. L., and Ding, J.: Kinetics and mechanism of heterogeneous oxidation of sulfur dioxide by ozone on surface of calcium carbonate, Atmos. Chem. Phys., 6, 2453–2464, doi:10.5194/acp-6-2453-2006, 2006.

Li, W. J. and Shao, L. Y.: Observation of nitrate coatings on atmospheric mineral dust particles, Atmos. Chem. Phys., 9, 1863–1871, doi:10.5194/acp-9-1863-2009, 2009.

Mogili, P. K., Kleiber, P. D., Young, M. A., and Grassian V. H.: Heterogeneous Uptake of Ozone on Reactive Components of Mineral Dust Aerosol: An Environmental Aerosol Reaction Chamber Study, J. Phys. Chem. A, 110, 13799–13807, 2006.

Ndour, M., D'anna, B., George, C., Ka, O., Balkanski, Y., Kleffmann, J., Stemmler, K., and Ammann, M.: Impact of the photocatalytic properties of mineral dust on atmospheric composition, Geoph. Res. Lett., 35, L05812, doi:10.1029/2007GL032006, 2008.

Pradhan, M., Kalberer, M., Griffiths, P. T., Braban, C. F., Pope, F. D., Cox, R. A., and Lambert, R. M.: Uptake of gaseous hydrogen peroxide by submicrometer titanium dioxide aerosol as a function of relative humidity, Environ. Sci. Technol., 44, 1360–1365, 2010a.

Pradhan, M., Kyriakou, G., Archibald, A. T., Papageorgiou, A. C., Kalberer, M., and Lambert, R. M.: Heterogeneous uptake of gaseous hydrogen peroxide by Gobi and Saharan dust aerosols: a potential missing sink for H_2O_2 in the troposphere, Atmos. Chem. Phys., 10, 7127–7136, doi:10.5194/acp-10-7127-2010, 2010b.

Prospero, J. M.: Long-range transport of mineral dust in the global atmosphere: Impact of African dust on the environment of the southeastern United States, Proc. Natl. Acad. Sci. USA, 96, 3396–3403, 1999.

Putaud, J.-P., Van Dingenen, R., Dell'Acqua, A., Raes, F., Matta, E., Decesari, S., Facchini, M. C., and Fuzzi, S.: Size-segregated aerosol mass closure and chemical composition in Monte Cimone (I) during MINATROC, Atmos. Chem. Phys., 4, 889–902, doi:10.5194/acp-4-889-2004, 2004.

Raff, J. D., Szanyi, J., and Finlayson-Pitts, B. J.: Thermal and photochemical oxidation of self-assembled monolayers on alumina particles exposed to nitrogen dioxide, Phys. Chem.

ACPD
11, 28563–28586, 2011

Chem. Phys., 13, 604–611, 2011.
Reeves, C. E. and Penkett, S. A.: Measurements of peroxides and what they tell us, Chem. Rev., 103, 5199–5218, 2003.
Schuttlefield, J., Rubasinghege, G., El-Maazawi, M., Bone, J., and Grassian, V. H.: Photochemistry of Adsorbed Nitrate, J. Am. Chem. Soc., 130, 12210–12211, 2008.
Sokolik, I. N. and Toon, O. B.: Direct radiative forcing by anthropogenic airborne mineral aerosols, Nature, 381, 681–683, 1996.
Sullivan, R. C., Guazzotti, S. A., Sodeman, D. A., and Prather, K. A.: Direct observations of the atmospheric processing of Asian mineral dust, Atmos. Chem. Phys., 7, 1213–1236, doi:10.5194/acp-7-1213-2007, 2007.
Surratt, J. D., Chan, A. W. H., Eddingsaas, N. C., Chan, M. N., Loza, C. L., Kwan, A. J., Hersey, S. P., Flagan, R. C., Wennberg, P. O., and Seinfeld, J. H.: Reactive intermediates revealed in secondary organic aerosol formation from isoprene, Proc. Natl. Acad. Sci., USA, 107, 6640–6645, 2010.
Ullerstam, M., Vogt, R., Langer, S., and Ljungstrom, E.: The kinetics and mechanism of SO_2 oxidation by O_3 on mineral dust, Phys. Chem. Chem. Phys., 4, 4694–4699, 2002.
Usher, C. R., Al-Hosney, H., Carlos-Cuellar, S., and Grassian, V. H.: A laboratory study of the heterogeneous uptake and oxidation of sulfur dioxide on mineral dust particles, J. Geophys. Res., 107, 4713, doi:10.1029/2002JD002051, 2002.
Usher, C. R., Michel, A. E., and Grassian, V. H.: Reactions on mineral dust, Chem. Rev., 103, 4883–4939, 2003a.
Usher, C. R., Michel, A. E., Steca, D., and Grassian, V. H.: Laboratory studies of ozone uptake on processed mineral dust, Atmos. Environ., 37, 5337–5347, 2003b.
Zhao, Y., Chen, Z. M., Shen, X. L., and Zhang, X.: Kinetics and Mechanisms of Heterogeneous Reaction of Gaseous Hydrogen Peroxide on Mineral Oxide Particles, Environ. Sci. Technol., 45, 3317–3324, 2011.

ACPD
11, 28563–28586, 2011

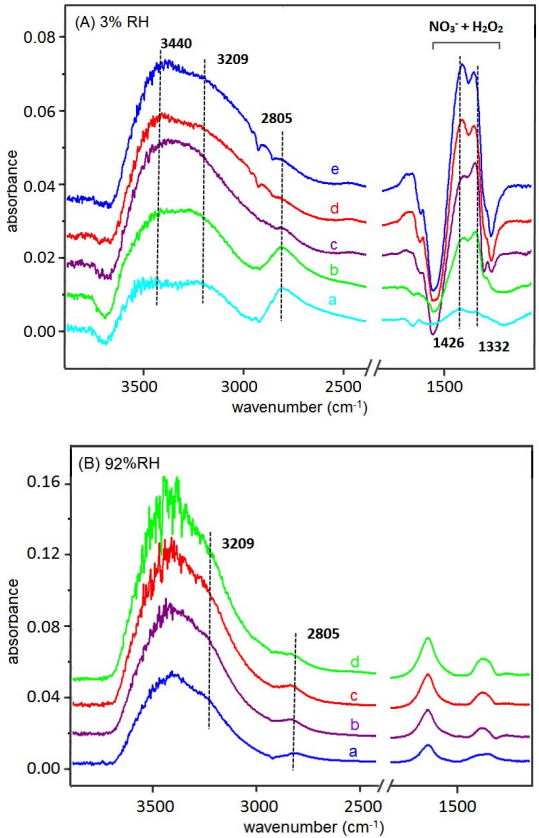

Fig. 1. T-FTIR spectra of H_2O_2 uptake on nitric acid-processed alumina particles with increasing nitrate coverage at **(A)** 3 % and **(B)** 92 %RH. **a**, **b**, **c**, **d**, and **e** in **(A)** correspond to surface nitrate coverage of 0, 1.1, 1.7, 2.7, and 3.5×10^{18} molecules m^{-2}, respectively. **a**, **b**, **c**, and **d** in **(B)** correspond to surface nitrate coverage of 0, 1.9, 2.6, and 3.2×10^{18} molecules m^{-2}, respectively. All of spectra were collected after 30 min of exposure.

ACPD
11, 28563–28586, 2011

Importance of atmospheric aging in reactivity of mineral dust aerosol

Y. Zhao et al.

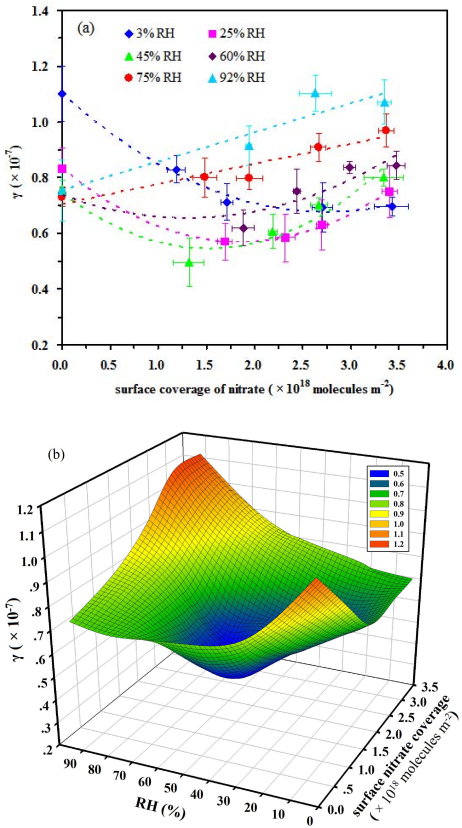

Fig. 2. The measured uptake coefficients of H_2O_2 on nitric acid-processed alumina particles as a function of RH and surface nitrate coverage. The measured uptake of H_2O_2 on clean alumina surfaces was also given for comparison. 3-D plot shown in **(b)** was derived based on the uptake data displayed in **(a)**. All of the uptake experiments were performed with 1.7×10^{14} molecules cm^{-3} gaseous H_2O_2.

ACPD
11, 28563–28586, 2011

CC BY

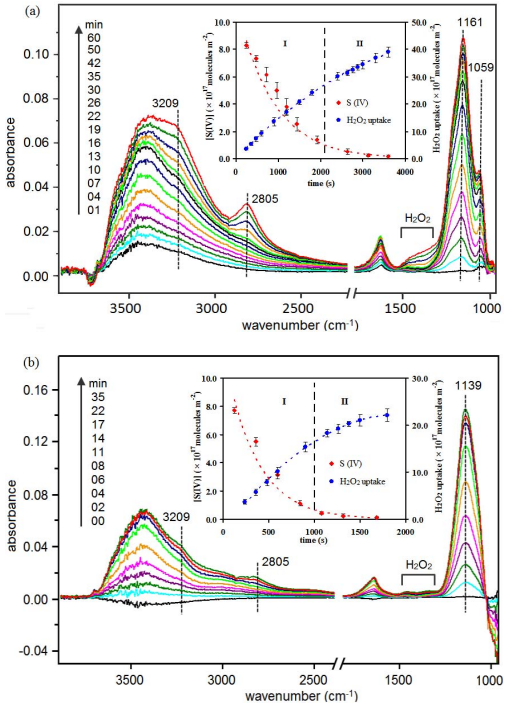

Fig. 3. T-FTIR spectra of SO_2-processed alumina particles recorded following exposure to 1.7×10^{14} molecules cm^{-3} gaseous H_2O_2 at RH of **(a)** 3 % and **(b)** 45 %. The insets show the uptake of H_2O_2 as well as the oxidation of surface S(IV) species as a function of time, and the data were normalized by the BET surface area of the particle samples. The S(IV) oxidation was derived from the formation of sulfate, which were determined using the integrated absorbance between 1350 and 1020 cm^{-1}.

ACPD
11, 28563–28586, 2011

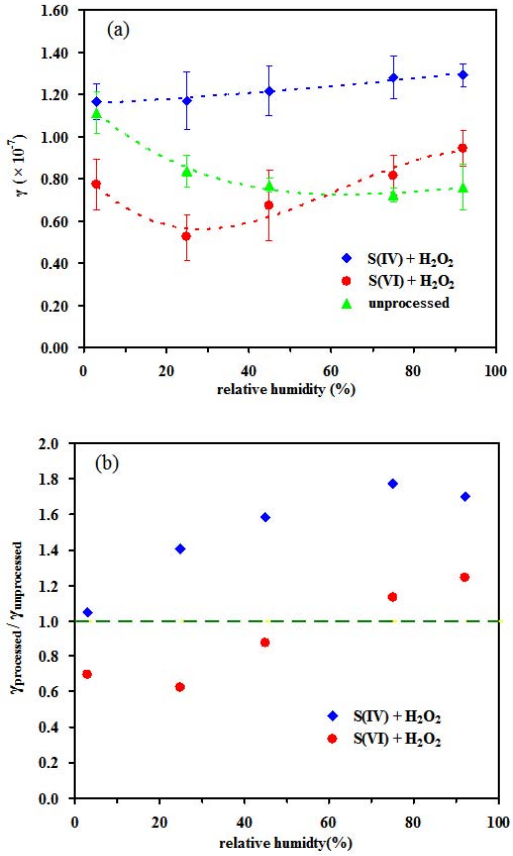

Fig. 4. Relative humidity dependence of the uptake coefficients of H_2O_2 on SO_2-processed alumina particles at different stages (I and II). The uptake of H_2O_2 on unprocessed alumina was also given for comparison. All of the experiments were conducted with 1.7×10^{14} molecules cm^{-3} gaseous H_2O_2.

ACPD
11, 28563–28586, 2011

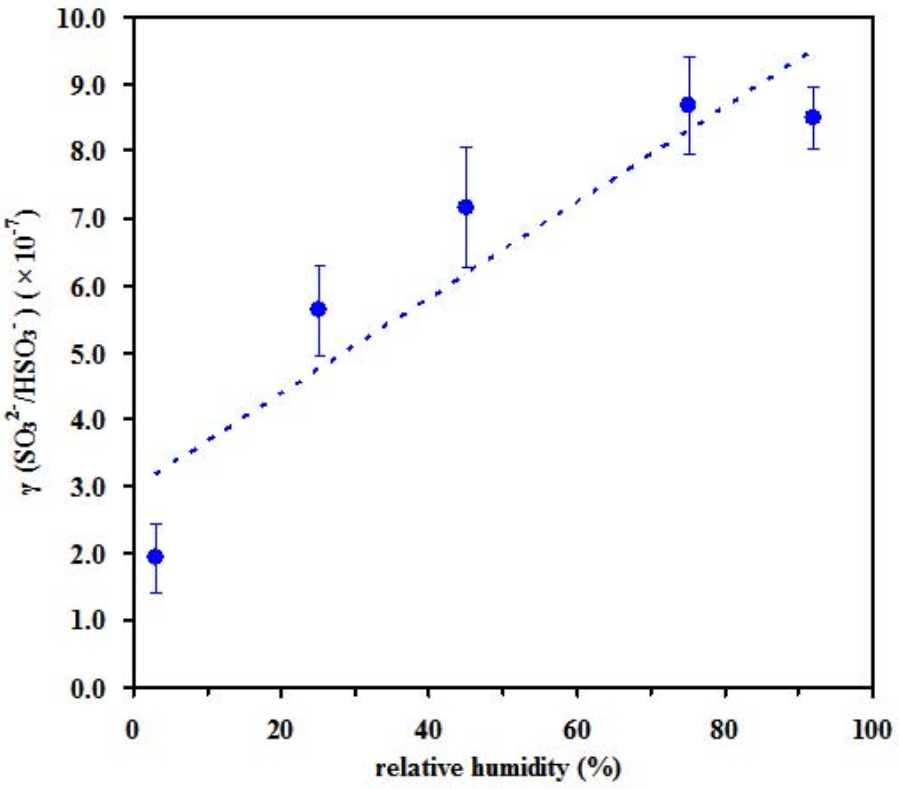

Fig. 5. The probability of oxidation of S(IV) to S(VI) by H_2O_2 on α-Al_2O_3 particles as a function of RH.

ACPD
11, 28563–28586, 2011